Hindawi
Advances in Meteorology
Volume 2023, Article ID 5519469, 10 pages
https://doi.org/10.1155/2023/5519469

Research Article

Study on O_3 Variations in Nanjing and the Surrounding Source Analysis

Jiaqi Shi,[1,2,3,4,5] **Jinhu Wang**,[1,2,3,4,5] **Yuqing Zhang**,[1,2,3] **Dinyuan Liang**,[1,2,3] **and Anhong Xiao**[1,2,3,4,5]

[1]*School of Emergency Management, Nanjing University of Information Science and Technology, Nanjing, Jiangsu 210044, China*
[2]*Collaborative Innovation Center on Forecast and Evaluation of Meteorological Disasters, Nanjing University of Information Science and Technology, Nanjing, Jiangsu 210044, China*
[3]*Key Laboratory of Middle Atmosphere and Global Environmental Observation, Chinese Academy of Sciences, Beijing 100029, China*
[4]*Academy of Disaster Reduction and Emergency Management of Nanjing University of Information Science and Technology, Nanjing, Jiangsu 210044, China*
[5]*Nanjing Xinda Institute of Safety and Emergency Management, Nanjing, Jiangsu 210044, China*

Correspondence should be addressed to Jinhu Wang; goldtigerwang@nuist.edu.cn

Received 26 July 2023; Revised 29 September 2023; Accepted 7 October 2023; Published 20 October 2023

Academic Editor: Maria Ángeles García

To understand the transport patterns and major sources of ozone (O_3) in Nanjing, this study carried out the 48-hour backward trajectories of air masses in Nanjing from March 2021 to March 2022, based on the HYSPLIT backward trajectory model driven by GDAS global reanalysis data. The primary transmission routes and putative source locations of O_3 pollution in Nanjing were determined through the integration of trajectory clustering analysis, potential source contribution function (PSCF), and concentration-weighted trajectory (CWT) analysis with meteorological data and O_3 concentration data. The results showed that the high O_3 concentrations and exceedance rates in Nanjing were in late spring and early summer, with the highest in June. The diurnal variation of O_3 concentrations in all seasons exhibited a single peak with a maximum from 13:00 to 16:00. The southeasterly flow passing through Zhenjiang, Changzhou, Wuxi, Suzhou, and Shanghai dominated the O_3 pollution in Nanjing. The PSCF and CWT presented a high consistency of O_3 potential sources in Nanjing. Zhenjiang, Ma'anshan, Changzhou, Wuxi, Suzhou, and Huzhou were identified as the main potential source regions of O_3 pollution in Nanjing. This study provides accurate theoretical references for regional joint prevention and control of O_3 pollution in Nanjing.

1. Introduction

O_3 is typically distributed in the stratosphere of the atmosphere to create the O_3 layer, which is a significant component of the atmosphere. The earth's biodiversity and the biological environment's stability can be efficiently protected by the O_3 layer's ability to absorb and block UV rays [1]. But in the troposphere, O_3 is a significant atmospheric contaminant. It is a secondary pollutant produced by intricate photochemical processes involving VOCs and NOx precursors. Both human health and the environment will suffer greatly from high O_3 concentrations [2].

In recent years, with the implementation of China's particulate matter prevention and control strategy, PM2.5-led particulate matter pollution has gradually reduced, but O_3 pollution has gradually increased, and O_3 has gradually replaced particulate matter as the primary air pollutant in most parts of China [3]. O_3, as a typical secondary pollutant, is more susceptible to regional transmission than particulate pollutants such as PM2.5. Hu et al. found in a study in the United States that particulate pollution such as PM2.5, as a primary emission and secondary pollutant, is affected by local influence up to 60%, regional transmission is only 10%, while O_3 concentration is affected by transmission [4]. China's

Yangtze River Delta region is economically developed, and industrial development is strong. It is also one of the regions with serious air pollution. Nanjing, as one of the core cities in the Yangtze River Delta region, is also seriously affected by air pollution.

The concentration of particulate matter pollution headed by PM2.5 in Nanjing has significantly dropped from 77 $\mu g \cdot m^{-3}$ in 2013 to 41 $\mu g \cdot m^{-3}$ in 2021 with the execution of the energy conservation and emission reduction strategy. However, the O_3 concentration has increased instead of decreasing, which has replaced PM2.5 as the first factor affecting air quality in Nanjing [5]. According to Wang et al. analysis of the generation of O_3 in the Nanjing urban area using the OBM model, the O_3 concentration in the city was particularly high in the spring and summer and was mostly regulated by volatile precursor VOCs [6]. Saavedra et al. have shown that tropospheric O_3 has a long lifetime and can sometimes exist in the atmosphere for several days, so O_3 pollution has the effect of regional transmission [7]. More information on O_3 pollution in urban and suburban areas of Nanjing is provided in the aforementioned research, but there is a dearth of information on O_3 potential source areas in Nanjing, which makes it difficult to determine how to jointly prevent and control O_3 pollution in those areas of Nanjing. Therefore, it is particularly important to explore the O_3 pollution transmission channels and potential source areas in Nanjing.

The backward trajectory algorithm is a weather and environmental forecasting technology, which can be used to track the trajectory of aerosols and pollutants. It is usually used in environmental impact assessment and air pollution prevention and control. For example, Dimitriou and Kassomenos used backward trajectories to analyze the sources of O_3 pollution in Athens, mainly from the Balkans and Greece [8]. According to Qian et al.'s analysis using the backward trajectory and PSCF approach, the main regions where O_3 pollution in Ganzhou City could have originated were Guangdong, Anhui, and northern Jiangxi [9]. Sharma et al. used PSCF and CWT methods to analyze that the potential source area of O_3 pollution in the Ganges Plain of India, which is the Delhi region of India [10]. According to Yang et al.'s analysis of the probable O_3 pollution source locations in the Anyang area using the PSCF approach, there were significant seasonal variations in O_3 pollution. For instance, in the summer, the industrial parks around Anyang, southern Hebei, and northern Hubei were the key locations of the prospective source areas. Long-distance transportation in Shanxi and northern Ezhou was the key factor affecting it in the autumn [11].

This paper uses backward trajectory technology, PSCF, and CWT methods to study the O_3 pollution transmission channel and its potential source area in the Nanjing area, based on data from air quality monitoring stations and meteorological data in 2021. The goal is to provide theoretical support for air quality forecasting and O_3 pollution prevention and control in the core cities of the Yangtze River Delta region.

2. Data and Methods

2.1. Air Quality and Meteorological Data. The 13 state-owned environmental quality monitoring stations in Nanjing (Maigaoqiao, Caochangmen, Shanxi Road, Zhonghuamen, Ruijin Road, Xuanwu Lake, Pukou, Olympic Sports Center, Xianlin University Town, Jiangning Rainbow Bridge, Lishui Yongyang, Gaochun Old Vocational School, and Liuhe Xiongzhou) (Figure 1) provided the ozone (O_3) hourly concentration data. The basic data of the ground-based weather stations are obtained from the China Meteorological Data Network including hourly average temperature, wind speed, and wind direction. The backward trajectory simulation uses data from the Global Data Assimilation System (GDAS) data provided by the National Centers for Environmental Prediction (NCEP) from 25 March, 2021, to 5 April, 2022, with a spatial resolution of $0.5^\circ \times 0.5^\circ$.

2.2. Backward Trajectory Model. The backward trajectory model (HYSPLIT) is one of the main methods for studying atmospheric pollutants. The model was jointly developed by the Air Resources Laboratory of the National Oceanic and Atmospheric Administration and the Australian Bureau of Meteorology. It is employed to compute and examine the diffusion and transport trajectories of air contaminants. The "HYSPLIT" model and "GIS" technologies are combined in the TrajStat software to calculate and analyze air mass trajectories [12].

In this study, the trajectory of O_3 pollutants in Nanjing, which is located at 32.04°N and 118.76°E, was calculated and examined using TrajStat software. The backward airflow trajectory is set to 48 hours, and the starting height of the trajectory is 500 meters above the ground. The airflow trajectory can correctly reflect the characteristics of the near-surface air mass trajectory at a height of 500 m since the surface has little impact on the airflow trajectory at this altitude. To concentrate on the impact of pollutant transport from neighboring cities to Nanjing, a 48-hour backward trajectory was estimated [13].

2.3. Trajectory Custer Analysis. The backward trajectory model is used to calculate a large number of trajectories, which are then clustered and analyzed. A total of 8715 48-hour backward trajectories from 1 March, 2021, to 28 February, 2022, were calculated in this paper. Euclidean distance was selected as the clustering method, and the trajectory clustering analysis was carried out in different seasons to obtain the pollution transmission path in different seasons, which was divided into spring (March–May), summer (June–August), autumn (September–November), and winter (December–February of the following year).

2.4. Potential Source Contribution Analysis. The study region is divided into $(i * j)$ grids using the potential source contribution function (PSCF), a method based on the conditional probability function. The PSCF value of each grid is calculated along with pollutant data and air mass

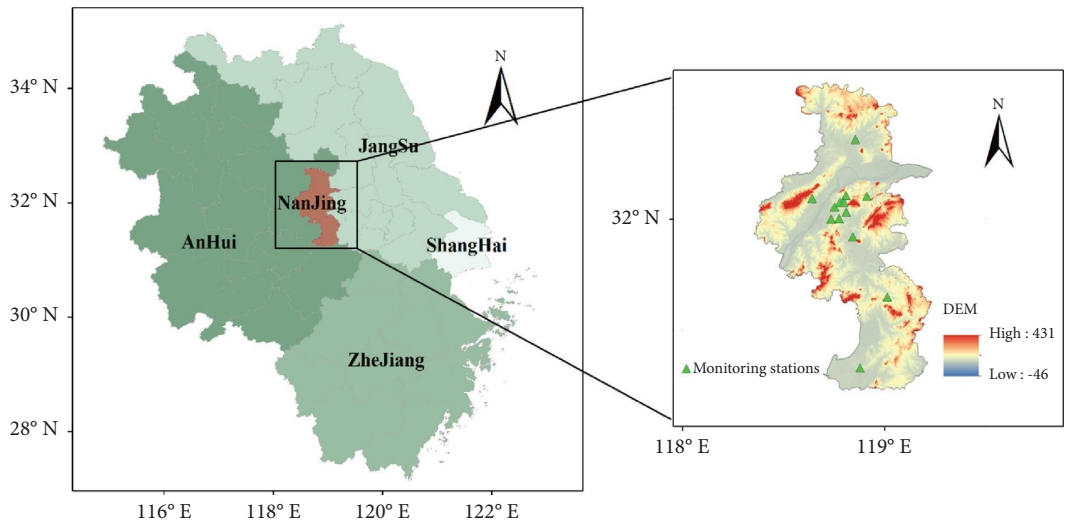

Figure 1: Geographical location of Nanjing in eastern China and detailed sites of ambient air quality monitoring with corresponding topographic elevations.

backward trajectory to assess the grid area's contribution to pollution in the research area.

$$\mathrm{PSCF}_{ij} = \frac{m_{ij}}{n_{ij}}. \quad (1)$$

In formula (1), "m_{ij}" refers to the number of trajectory nodes that the pollutant exceeds the concentration threshold in a grid, and "n_{ij}" is the number of nodes of all trajectories in the grid [14]. The threshold of the trajectory node in this study is determined as the MDA8 O_3 concentration surpassing the secondary pollution level of 160 $\mu g/m^{-3}$. The results may be incorrect if there are few pollution pathway nodes in the grid, as the PSCF is a conditional probability function [15]. To lessen the impact of inaccuracy, the WPSCF method is implemented, which adds the weight coefficient W_{ij}, as given in the following formula:

$$\mathrm{WPSCF}_{ij} = \frac{m_{ij}}{n_{ij}} W_{ij}. \quad (2)$$

The weight coefficient is based on the number of pollution trajectory nodes, as given in the following formula:

$$W_{ij} = \begin{cases} 1.00\ 120 < n_{ij}, \\ 0.7\ 30 < n_{ij} \le 120, \\ 0.42\ 15 < n_{ij} \le 30, \\ 0.05\ n_{ij} \le 15. \end{cases} \quad (3)$$

2.5. Concentration-Weighted Trajectory. This approach can only provide the distribution of the pollutant's possible source area and cannot indicate the degree to which the potential source area pollution is contributing because PSCF determines whether a trajectory in the grid is contaminated based on the established pollutant threshold. In order to express the contribution of pollutant concentration in various pollution source areas, the concentration trajectory weighting (CWT) approach is introduced. The region's real pollution concentration is communicated at a higher rate with a bigger CWT value than it is with a smaller one, or vice versa, as given in the following equation [2]:

$$C_{ij} = \frac{\sum_{l=1}^{M} C_l \cdot \tau_{ijl}}{\sum_{l=1}^{M} \tau_{ijl}}. \quad (4)$$

In the above formula, "C_{ij}" is the average weight concentration of the grid (i, j), "l" is the trajectory, "M" is the number of trajectories, "C_l" is the O_3 concentration corresponding to the trajectory "l" passing through the grid (i, j), and "τ_{ijl}" is the residence time of the trajectory "l" in the grid. Similarly, in order to reduce the influence of the small value of "n_{ij}", the weight coefficient "W_{ij}" is multiplied by CWT to reduce the uncertainty, where the weight coefficient "W_{ij}" is the same as PSCF weight coefficient [16].

3. Results and Analysis

3.1. Variations in O_3 and Pollution. In Figure 2, the time series of the mean surface daily maximum 8-hour average (MDA8) O_3 concentration in Nanjing from spring 2021 to spring 2022 is described. It can be seen that the concentration range is between 37 and 236 $\mu g{\cdot}m^{-3}$, and the fluctuation range is mainly concentrated between the first-level concentration standard (100 $\mu g{\cdot}m^{-3}$) and the second-level concentration standard (160 $\mu g{\cdot}m^{-3}$) of MDA8 O_3, among which the number of pollution days exceeding the second-level standard limit of 160 $\mu g{\cdot}m^{-3}$ reaches 59 days.

Figure 3 shows the monthly average O_3 concentration distribution and the over-standard rate of the secondary pollution standard. It is clear that Nanjing's O_3 pollution exhibits distinct seasonal patterns. Late spring and early summer are the seasons with the highest concentrations of O_3, followed by early fall and winter with the lowest concentrations. The MDA8 O_3 exceedance rates at each month in Nanjing characterize summer (28.2%) > spring (23.3%)

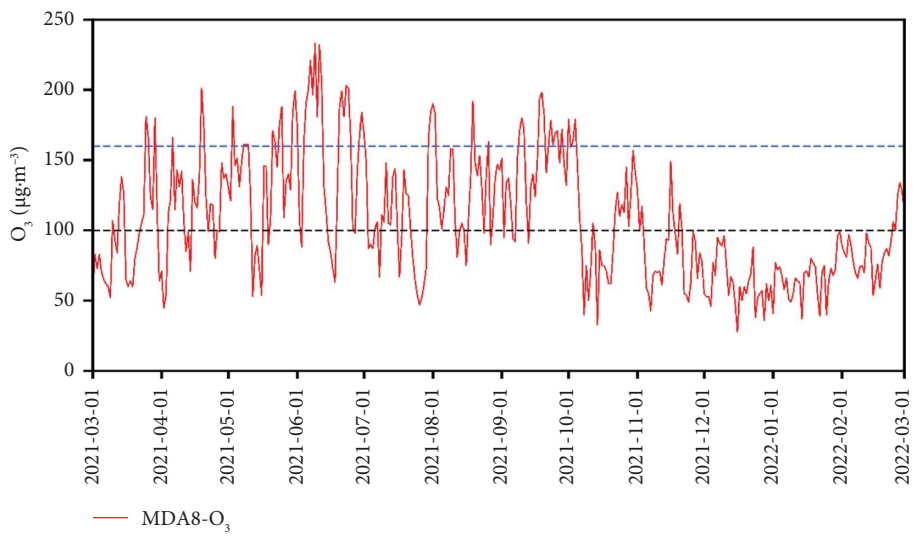

Figure 2: Time series of MDA8 O3 in Nanjing from 1 March, 2021, to 1 March, 2022. Black and blue dashed line, respectively, represent O_3 primary and secondary pollution standards.

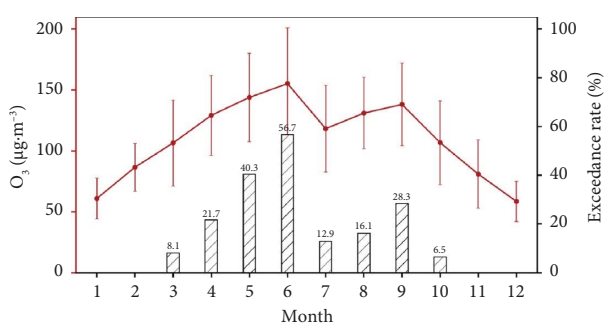

Figure 3: Observed monthly mean O_3 concentrations (units) in Nanjing during 1 March, 2021, to 1 March, 2022 and the corresponding exceedance rate (%).

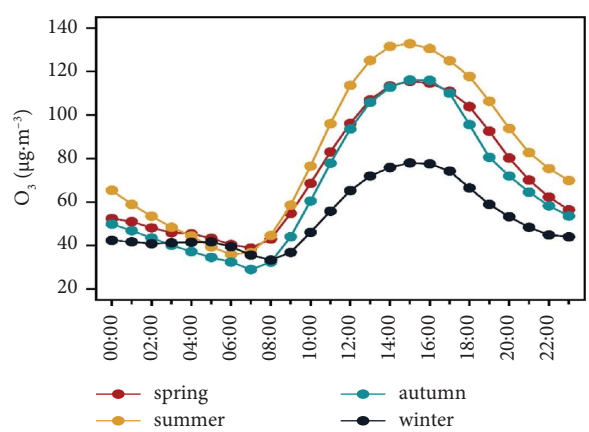

Figure 4: Diurnal variations in O_3 concentrations average over each season in Nanjing during 1 March, 2021, to 1 March, 2022.

> autumn (11.5%) > winter (no exceeding standard), with the severest pollution in summer (Figure 3). The summer months saw the highest exceedance rates, notably 56.7% in June. This was mostly because the O_3 concentration increased during these months due to increased solar radiation, higher surface temperatures, and reduced relative humidity. In contrast, there were no exceedances of O_3 concentrations in winter, which is due to lower temperatures, shorter sunshine hours, weaker solar radiation, and high relative humidity that are not conducive to the formation of O_3 [17].

A deeper examination of the diurnal fluctuation of O_3 concentration in Nanjing during the various seasons (Figure 4) reveals that it is a single peak type, with summer being the season with the highest peak concentration and winter being the season with the lowest. Each season's peak concentration time is nearly the same (13:00–16:00), and the valley concentration phase is between 6:00 and 8:00. This is due to the fact that the O_3 is produced to raise the concentration of the photochemical reaction, which is intense during the day. O_3 is depleted by the titration of NO at night until the solar radiation increases once more in the early morning hours of the next day, at which point the O_3 concentration gradually rises once more [18].

3.2. Analysis of Pollutant Transmission Paths in Different Seasons. 8715 airflow trajectories in the Nanjing area were examined in various seasons in order to reveal the near-surface transport characteristics of pollutant transport channels. The trajectory clustering analysis was conducted in various seasons, as shown in Figure 5, including four in summer and three in all other seasons. The transport paths, transport distances, and proportion of each airflow are provided in Table 1.

The southeast-eastward airflow (track 2) in Nanjing had the highest proportion (46.04%) in spring, followed by the northward airflow (track 1) and the southwest-westward airflow (track 3), which had respective shares of 27.28% and 26.68%. All three airflows moved more quickly.

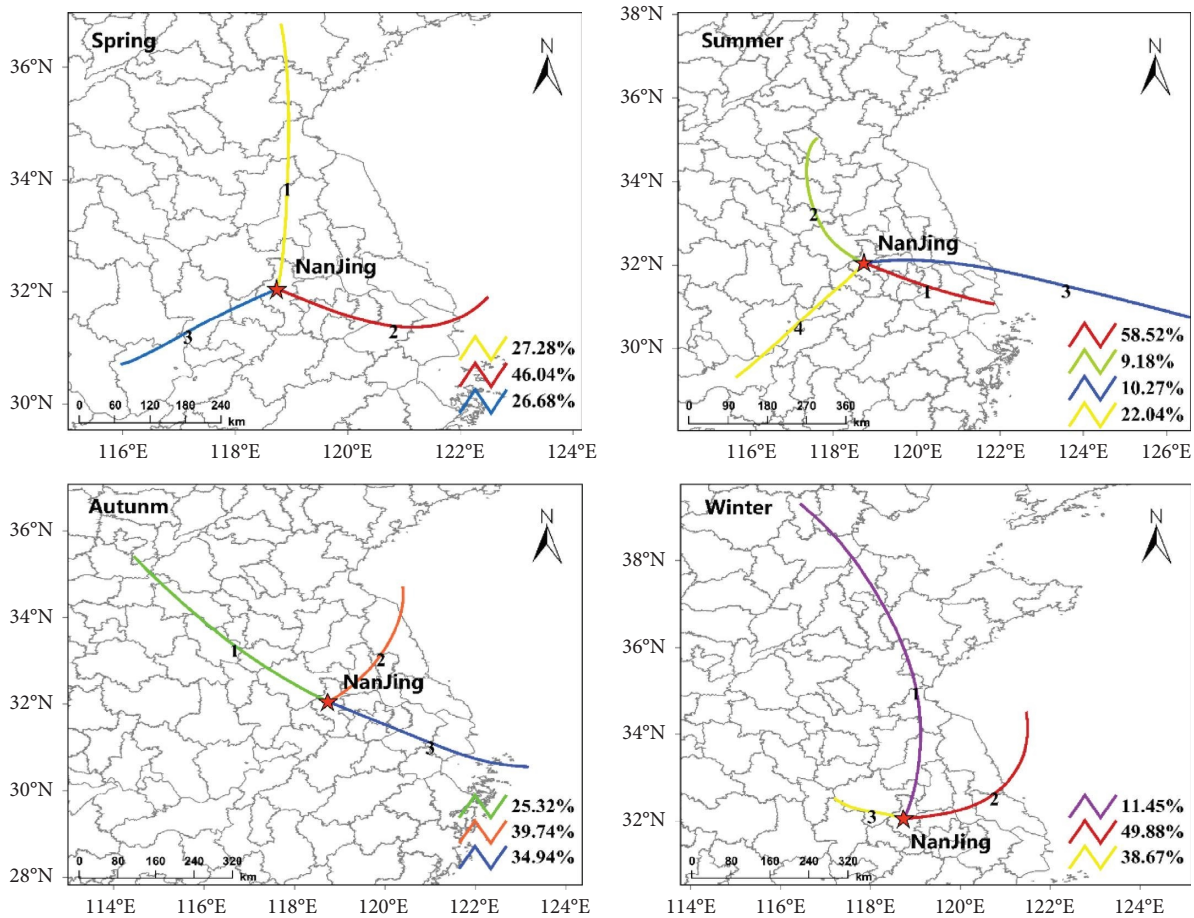

Figure 5: Cluster-mean back trajectories results for Nanjing.

In summer, Nanjing's predominant airflow originates from the southeast. There are two major airflow tracks in this direction (tracks 1 and 3), of which track 1 accounts for the largest proportion, 58.52%, and moves slowly, while track 2 accounts for a smaller proportion, 10.27%, and moves quickly. The airflow from the southwest (track 4) and northwest (track 2) accounted for 22.04% and 9.18%, respectively.

In autumn, the airflow in Nanjing mainly comes from the three directions of southeast, northeast, and northwest. All three airflows account for a relatively high proportion, the northeast airflow (track 2) accounts for the highest at 39.74%, the airflow speed is slow; southeast airflow (track 3) and northwest airflow (track 1) account for 34.94% and 25.32%, respectively.

In winter, the airflow in Nanjing mainly comes from the northeast direction (track 2), accounting for 49.88%, followed by the northwest westerly airflow (track 3) and northward air flow (track 1), accounting for 38.67% and 11.45%, respectively, of which the airflow of track 3 moves slowly and the airflow of track 1 moves faster.

In conclusion, based on the rose diagram of O_3 wind direction in different seasons in Nanjing shown in Figure 6, it is evident that during spring, high concentrations of O_3 mainly occur in the southeast to east-southeast wind directions (Figure 6(a)), followed by northeast and southwest to west-southwest wind directions. During summer, high concentrations of O_3 primarily appear in the southeast and east wind directions (Figure 6(b)), while during autumn, high concentrations of O_3 are mainly concentrated in the southeast wind direction (Figure 6(c)). During winter, O_3 concentrations are relatively low, but eastward winds can cause an increase in O_3 concentration (Figure 6(d)). According to the analysis, Nanjing's high O_3 concentrations in each season are mostly caused by southeast and east winds blowing upward, and the highest values of O_3 concentration are concentrated in the region of 4–8 m/s. The airflow trajectory through Zhenjiang, Changzhou, Wuxi, Suzhou, and other cities results in the same general pattern of O_3 pollution transmission channels in spring, summer, and autumn. In Nanjing, the airflow transfer in this direction is mostly responsible for O_3 pollution. The majority of the

Table 1: Pollution air mass tracks in spring, summer, autumn, and winter.

Season	Track	Track direction	Airflow trajectories area	Probability (%)	Distance (km)
Spring	Track 1	North	Weifang, Rizhao, Lianyungang, Suqian, Huaian, and east of Chuzhou	27.28	550
	Track 2	Southeast	Shanghai, Suzhou, Wuxi, Changzhou, and Zhenjiang	46.04	350
	Track 3	Southwest	North of Anqing, Hefei, and Ma'anshan	26.68	300
Summer	Track 1	Southeast	Shanghai, Suzhou, Wuxi, Changzhou, and Zhenjiang	58.52	350
	Track 2	Northwest	Zaozhuang, Xuzhou, Suzhou, Bengbu, and Chuzhou	9.18	380
	Track 3	Southeast-eastward	Central Yellow sea, Nantong, Taizhou, and Zhenjiang	10.27	750
	Track 4	Southwest	Border of Anqing and Jiujiang, Tonglin, Wuhu, and Ma'anshan	22.04	400
Autumn	Track 1	Northwest	Kaifeng, Shangqiu, Haozhou, Bengbu, and Chuzhou	25.32	500
	Track 2	Northeast	North of Yellow sea, Yancheng, and Yangzhou	39.74	300
	Track 3	Southeast	Border of Yellow sea and east China sea, Shanghai, Suzhou, Wuxi, and Zhenjiang	34.94	400
Winter	Track 1	North	Langfang, Cangzhou, Binzhou, Weifang, east of Linyi, Liangyungang, Huaian, and east of Chuzhou	11.45	800
	Track 2	Northeast-eastward	Central Yellow sea, North of Nantong, Taizhou, and Zhenjiang	49.88	350
	Track 3	West	Border of Chuzhou and Hefei	38.67	100

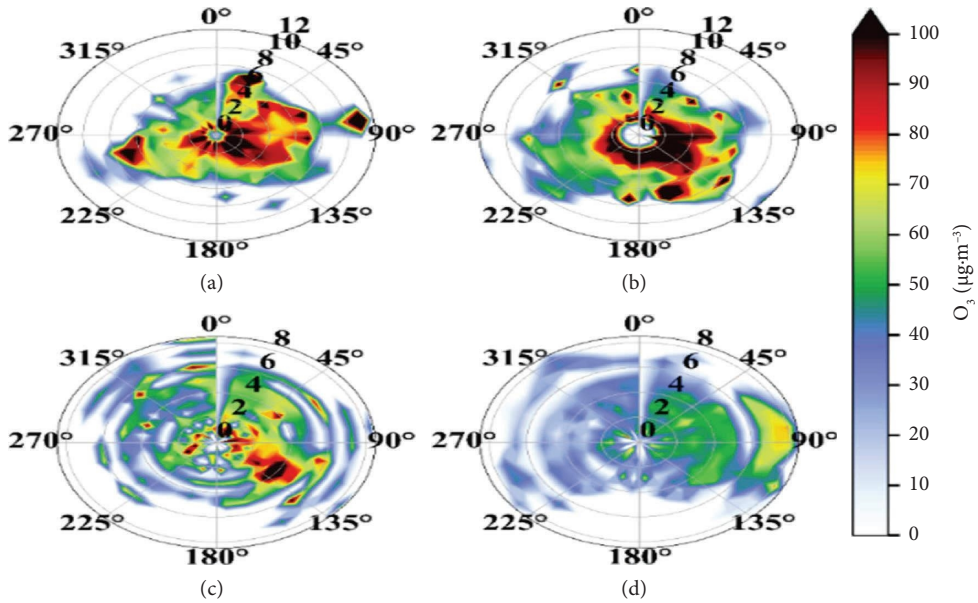

Figure 6: Relationship between wind speed and wind direction on O_3 concentration in Nanjing. (a) spring, (b) summer, (c) autumn, (d) winter.

cities in this direction are economically developed cities in the Yangtze River Delta region, with significant levels of anthropogenic and industrial emissions, which cause a series of photochemical reactions to produce large concentrations of O_3 as a result.

3.3. Analysis of Potential Source Areas and Their Contributions. The WPSCF approach was used to examine the possible source areas of O_3 pollution in different seasons in Nanjing in order to further determine the geographical distribution of the potential source areas of O_3 pollution. Figure 7 depicts the results of the WPSCF analysis. There are significant seasonal changes in the distribution of potential O_3 pollution source sites in Nanjing; however, the main potential source locations are concentrated in the city's surrounding and southeastern districts.

The high probability of O_3 pollution source area in Nanjing in spring is the high-value area of WPSCF (WPSCF >0.5) at the junction of southern Nanjing and Ma'anshan, and the secondary high-value (WPSCF >0.4) areas of Changzhou and Wuxi, as well as Huzhou and Jiaxing in northern Zhejiang. In summer, the high-value area of WPSCF (WPSCF >0.53) is the largest, mainly concentrated in Zhenjiang, Jiaxing, Zhejiang, Wuxi, Changzhou, Suzhou, Huzhou, and other places in the southeast of Nanjing. The large area in the southeast of Nanjing has a great probability to be the key source of O_3 pollution in Nanjing in the summer. The key source areas of O_3 pollution in Nanjing in autumn are mainly concentrated in the surrounding areas of Nanjing with high WPSCF values (WPSCF >0.4), as well as Ma'anshan, Wuhu, Xuancheng, and other areas in Anhui Province. In winter, the WPSCF value is significantly lower than that in spring, summer, and autumn, and the high-value area (WPSCF >0.1) in Hefei, Chuzhou, and other places in Anhui Province has only a small probability of being a potential source of O_3 pollution.

The PSCF approach calculates the probability that a specific location could be an O_3 pollution source. The CWT approach is used to examine the contribution of the probable source area to O_3 concentration in Nanjing in order to further explore the level of contribution of O_3 pollution in Nanjing. The outcomes of the WCWT analysis are shown in Figure 8.

When combined with the findings of the WPSCF and WCWT analyses, there are similarities between the two approaches in terms of the distribution area, but WCWT clearly indicates the level of possible source area contribution to O_3 in the Nanjing area. The area's contribution increases with increasing WCWT values. The high-value area of O_3 concentration contribution (WCWT >90 μg·m^{-3}) in the spring was consistent with the potential source area obtained by WPSCF analysis. The high-value area of concentration contribution was mainly concentrated in the south of Nanjing to Ma'anshan in Anhui, Changzhou, Wuxi, and Huzhou in Zhejiang, among which the concentration contribution in the south of Nanjing reached 108.2 μg·m^{-3}. In summer, the high-value areas of O_3 concentration contribution are more widely distributed than the high-value areas of potential source areas analyzed by WPSCF, but the regions are basically the same. The high-value areas are located in Zhenjiang, Changzhou, Wuxi, and Suzhou in eastern Nanjing and Huzhou, and Jiaxing in Zhejiang. The concentration contribution at the junction of Wuxi, Changzhou, and Huzhou is as high as 138.5 μg·m^{-3}. The high-value area of O_3 concentration contribution in autumn is basically consistent with the high-value area of WPSCF potential source area, and the concentration contribution value in the southeast of Nanjing is 83.7 μg·m^{-3}. In winter, some low-concentration O_3 source areas are located

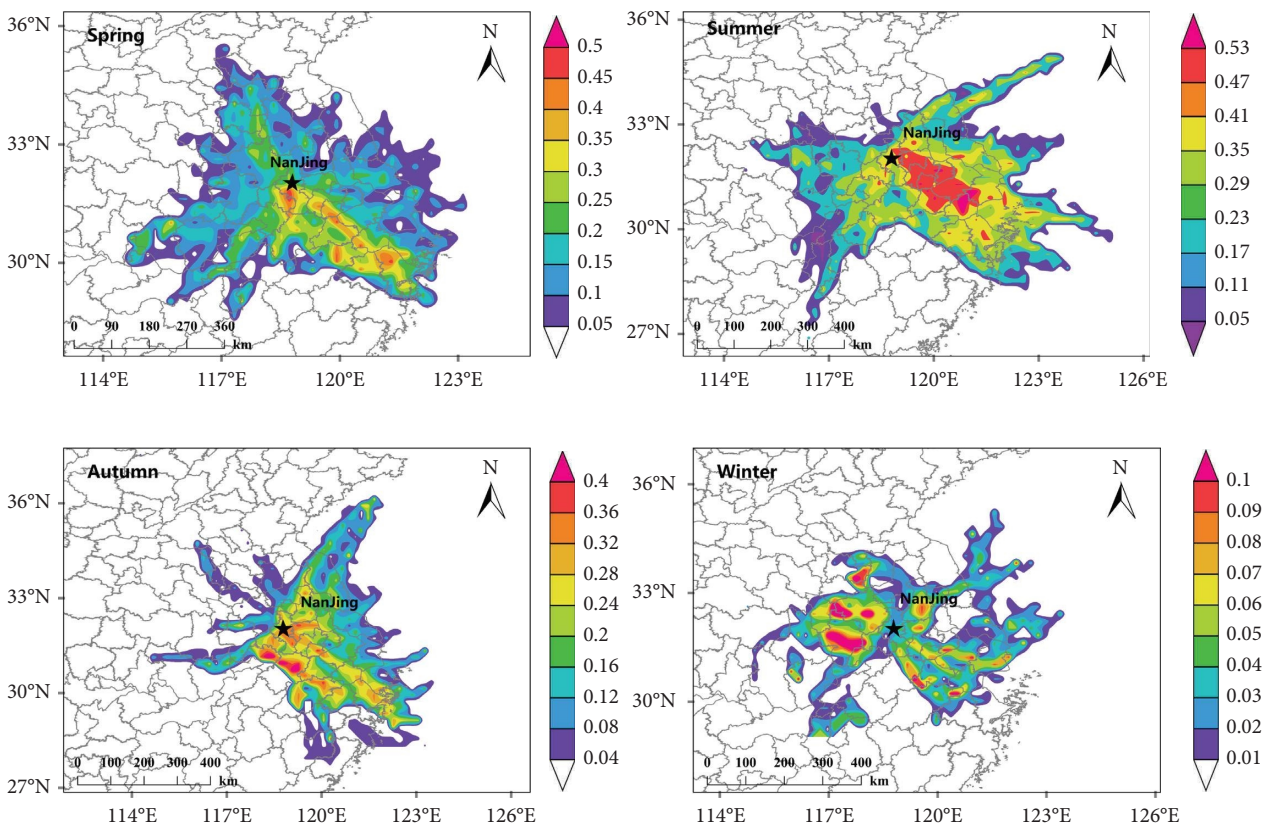

Figure 7: The spatial distributions of the WPSCF on Nanjing O_3 in spring, summer, autumn, and winter.

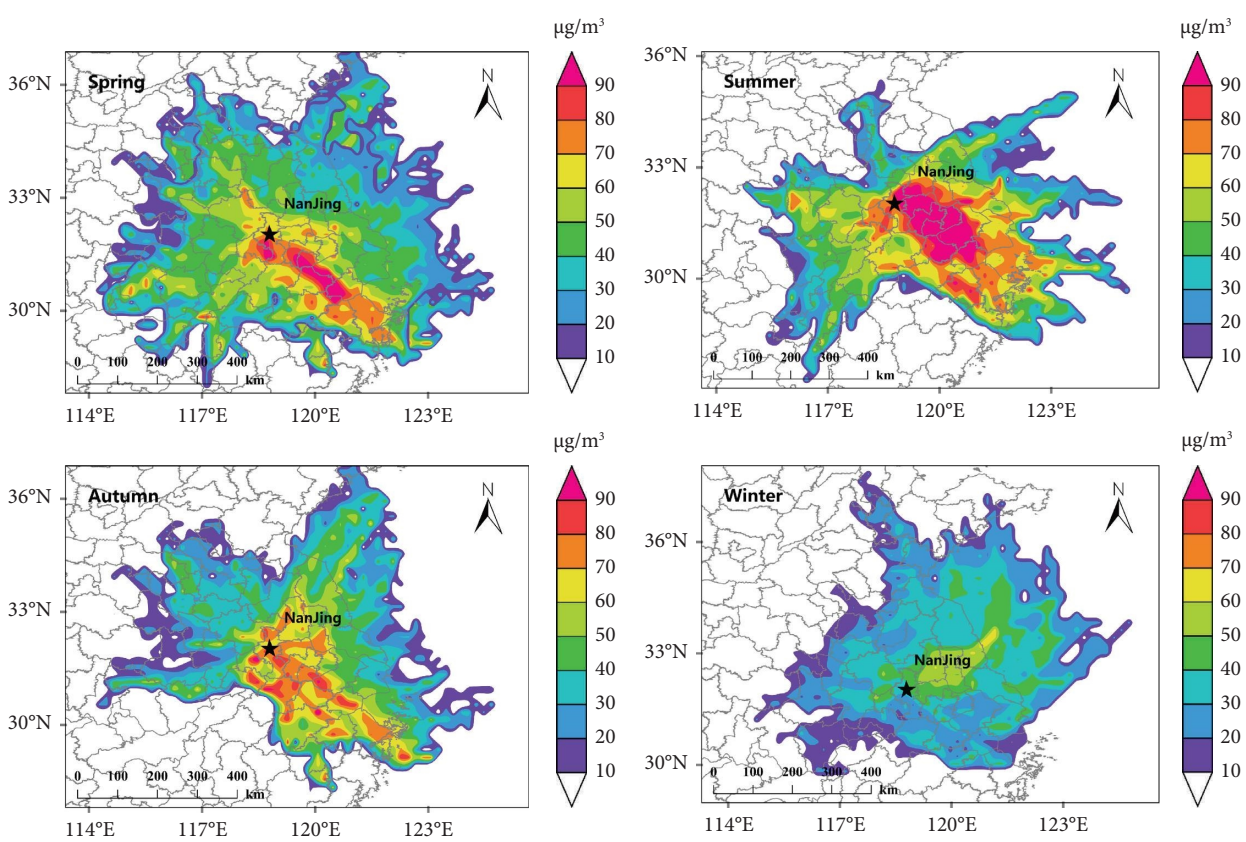

Figure 8: The outcomes of the WCWT analysis.

in the northeast of Nanjing. The distribution of the WCWT source area and the WPSCF source area in winter is quite different. This is due to the low O_3 concentration in winter, which is difficult to reach the pollution concentration threshold in the PSCF method.

The possible contribution of the surrounding areas to O_3 pollution in Nanjing was investigated using WPSCF and WCWT analysis methodologies. Although there were minor variations in the distribution range, the source area distribution was essentially the same. The outcomes of the two analyses generally agreed well. The distribution of high-value areas of O_3 pollution potential sources and high-value areas of O_3 concentration contribution was not in Nanjing, indicating that O_3 pollution in Nanjing was greatly affected by cross-regional transmission. The southeast of Nanjing is where most of the city's high-value locations of potential sources of O_3 pollution and high-value areas of O_3 concentration contribution in other seasons are concentrated, in addition to the winter months with reduced O_3 pollution. This is mostly because the high-value sites are situated in the Yangtze River Delta's economically developed regions, which have significant levels of anthropogenic and industrial emissions, and where the emitted precursors are photochemically transformed into O_3 with high concentrations. O_3 pollution is more likely to spread regionally than particulate matter pollution [19], and Nanjing is situated in its downwind region. Therefore, transmission in these locations significantly impacts O_3 pollution in Nanjing.

4. Conclusions

(1) O_3 pollution in Nanjing was particularly bad in the spring and summer of 2021, with the O_3 concentration reaching its peak in late spring and early summer. Nanjing's O_3 exceeded the standard by 59 days, which is slightly more than the average level of Yangtze River Delta cities. The greatest number of days in which MDA8 O_3 levels were over the recommended level in June was 17 days, with the lowest average concentration in winter and no occurrence of pollution exceeding the standard. Every season had a single peak in the diurnal variation of MDA8 O_3 concentration, which arrived around 13:00 and disappeared around 7:00.

(2) A total of 8715 air mass transport trajectories reaching Nanjing in 2021 were analyzed by backward trajectory simulations. The main transport path of high-concentration O_3 pollution is southeastward through Changzhou, Wuxi, Suzhou, Huzhou, and other cities around Taihu Lake. The airflow trajectory of this transport path accounts for the highest proportion of 40.19%, followed by the southwest area through Ma'anshan, Anhui, Hefei, Ma'anshan, Wuhu, and other cities. The airflow trajectory of this path accounts for 32.42%. These two main airflow transport paths play a leading role in O_3 pollution in Nanjing.

(3) The two approaches of (PSCF and CWT) both produced high-value zones with good consistency. The results demonstrate that regional transmission has a significant impact on the O_3 pollution in the Nanjing area, but that the high-value areas generated by CWT analysis are more accurate than PSCF to give the contribution of individual source areas. Changzhou, Wuxi, Suzhou, Huzhou, and other areas around Taihu Lake in the southeast of Nanjing are the main potential source areas of O_3 pollution. The surrounding areas, such as Zhenjiang, Ma'anshan, Wuhu, and Hefei, also contribute to O_3 pollution in Nanjing. Therefore, to prevent and control O_3 pollution in Nanjing, it is necessary to strengthen the joint prevention and control of the Yangtze River Delta region, especially for the pollution emission control of the upper cities.

Data Availability

The data used and analyzed during the current study are available from the corresponding author upon reasonable request.

Conflicts of Interest

The authors declare that they have no conflicts of interest.

Acknowledgments

This work was supported by the National Natural Science Foundation of China (no. 41905026), the Natural Science Foundation of Jiangsu Province (no. BK20170945), and the Nanjing University of Information Science and Technology Talent Start-Up Foundation (no. 2016r028).

References

[1] S. E. Braslavsky and M. B. Rubin, "The history of ozone Part VIII. Photochemical formation of ozone," *Photochemical and Photobiological Sciences*, vol. 10, no. 10, pp. 1515–1520, 2011.

[2] C. H. Li, B. R. Mai, and Y. B. Li, "Study on transmission channel and pollution sources region of O_3 in qingyuan city," *Journal of Environmental and Public Health*, vol. 2022, Article ID 1837492, 12 pages, 2022.

[3] J. Wei, Z. Li, K. Li et al., "Full-coverage mapping and spatiotemporal variations of ground-level ozone (O_3) pollution from 2013 to 2020 across China," *Remote Sensing of Environment*, vol. 270, Article ID 112775, 2022.

[4] Y. T. Hu, M. T. Odman, A. G. Russell, N. Kumar, and E. Knipping, "Source apportionment of ozone and fine particulate matter in the United States for 2016 and 2028," *Atmospheric Environment*, vol. 285, Article ID 119226, 2022.

[5] F. J. Xie, X. B. Lu, F. Yang et al., "Transport influence and potential sources of ozone pollution for nanjing during spring and summer in 2017," *Environmental Sciences*, vol. 42, no. 1, pp. 88–96, 2021.

[6] M. Wang, W. T. Chen, L. Zhang et al., "Ozone pollution characteristics and sensitivity analysis using an observation-based model in Nanjing Yangtze River Delta Region of China," *Journal of Environmental Sciences*, vol. 93, pp. 13–22, 2020.

[7] S. Saavedra, A. Rodríguez, J. J. Taboada, J. A. Souto, and J. Casares, "Synoptic patterns and air mass transport during ozone episodes in northwestern Iberia," *Science of the Total Environment*, vol. 441, pp. 97–110, 2012.

[8] K. Dimitriou and P. Kassomenos, "Three year study of tropospheric ozone with back trajectories at a metropolitan and a medium scale urban area in Greece," *Science of the Total Environment*, vol. 502, pp. 493–501, 2015.

[9] Y. Qian, B. Xu, L. J. Xia et al., "Analysis of ozone pollution characteristics and influence of meteorological factors in Jiangxi Province from 2016-2019," *Environmental Sciences*, vol. 42, no. 5, pp. 2190–2201, 2021.

[10] A. Sharma, T. K. Mandal, S. K. Sharma, D. K. Shukla, and S. Singh, "Relationships of surface ozone with its precursors, particulate matter, and meteorology over Delhi," *Journal of Atmospheric Chemistry*, vol. 74, no. 4, pp. 451–474, 2017.

[11] J. Yang, S. S. Yin, S. J. Yu et al., "Characteristic of surface ozone and meteorological parameters analysis in Anyang City," *Environmental Sciences*, vol. 41, no. 1, pp. 115–124, 2020.

[12] Y. Q. Wang, X. Y. Zhang, and R. R. Draxler, "TrajStat: GIS-based software that uses various trajectory statistical analysis methods to identify potential sources from long-term air pollution measurement data," *Environmental Modelling & Software*, vol. 24, no. 8, pp. 938-939, 2009.

[13] Y. F. Zhu, J. Y. Liao, G. Wei et al., "Air pollutants sources in winter in chang-zhu-tan region of China," *Advances in Meteorology*, vol. 2022, Article ID 9717192, 12 pages, 2022.

[14] Y. H. Zhu, L. X. Yang, K. Kawamura et al., "Contributions and source identification of biogenic and anthropogenic hydrocarbons to secondary organic aerosols at Mt. Tai in 2014," *Environmental Pollution*, vol. 220, pp. 863–872, 2017.

[15] X. Xu and U. S. Akhtar, "Identification of potential regional sources of atmospheric total gaseous mercury in Windsor, Ontario, Canada using hybrid receptor modeling," *Atmospheric Chemistry and Physics*, vol. 10, no. 15, pp. 7073–7083, 2010.

[16] Y. Chen, S. Xie, and B. Luo, "Seasonal variations of transport pathways and potential sources of PM2.5 in Chengdu, China (2012-2013)," *Frontiers of Environmental Science & Engineering*, vol. 12, no. 1, 2018.

[17] T. H. Cao, H. C. Wang, L. Li, X. Lu, Y. M. Liu, and S. J. Fan, "Fast spreading of surface ozone in both temporal and spatial scale in Pearl River Delta," *Journal of Environmental Sciences*, vol. 137, no. 2, pp. 540–552, 2023.

[18] C. B. Baublitz, A. M. Fiore, O. E. Clifton et al., "Sensitivity of tropospheric ozone over the southeast USA to dry deposition," *Geophysical Research Letters*, vol. 47, no. 7, 2020.

[19] C. Huang, C. H. Chen, L. Li et al., "Anthropogenic air pollutant emission characteristics in the Yangtze River Delta region," *Journal of Environmental Sciences*, vol. 31, no. 9, pp. 1858–1871, 2011.